



Molecular Crystals and Liquid Crystals Science and Technology. Section A. Molecular Crystals and Liquid Crystals

Publication details, including instructions for authors and
subscription information:

<http://www.tandfonline.com/loi/gmcl19>

$M(\text{dmit})_2$ and $M(\text{dmise})_2$ ($M = \text{Ni}, \text{Pd}$) Compounds with One-, Two-and Three-Dimensional Metallic Bands

Akiko Kobayashi ^a, Akane Sato ^b, Toshio Naito ^b & Hayao
Kobayashi ^c

^a Department of Chemistry, School of Science, The University of
Tokyo, Hongo, Bunkyo-ku, Tokyo, 113, Japan

^b Department of Chemistry, Faculty of Science, Toho University
Funabashi, Chiba, 274, Japan

^c Institute for Molecular Science, Okazaki, 444, Japan

Version of record first published: 24 Sep 2006.

To cite this article: Akiko Kobayashi, Akane Sato, Toshio Naito & Hayao Kobayashi (1996):
 $M(\text{dmit})_2$ and $M(\text{dmise})_2$ ($M = \text{Ni}, \text{Pd}$) Compounds with One-, Two-and Three-Dimensional Metallic
Bands, *Molecular Crystals and Liquid Crystals Science and Technology. Section A. Molecular
Crystals and Liquid Crystals*, 284:1, 85-96

To link to this article: <http://dx.doi.org/10.1080/10587259608037913>

PLEASE SCROLL DOWN FOR ARTICLE

Full terms and conditions of use: <http://www.tandfonline.com/page/terms-and-conditions>

This article may be used for research, teaching, and private study purposes. Any
substantial or systematic reproduction, redistribution, reselling, loan, sub-licensing,
systematic supply, or distribution in any form to anyone is expressly forbidden.

The publisher does not give any warranty express or implied or make any
representation that the contents will be complete or accurate or up to date. The
accuracy of any instructions, formulae, and drug doses should be independently
verified with primary sources. The publisher shall not be liable for any loss, actions,

claims, proceedings, demand, or costs or damages whatsoever or howsoever caused arising directly or indirectly in connection with or arising out of the use of this material.

M(dmit)₂ AND M(dmise)₂ (M=Ni, Pd) COMPOUNDS WITH ONE-, TWO- AND THREE-DIMENSIONAL METALLIC BANDS

AKIKO KOBAYASHI*

Department of Chemistry, School of Science, The University of Tokyo,
Hongo, Bunkyo-ku, Tokyo 113, Japan

AKANE SATO AND TOSHIO NAITO

Department of Chemistry, Faculty of Science, Toho University
Funabashi, Chiba 274, Japan

HAYAO KOBAYASHI

Institute for Molecular Science, Okazaki 444, Japan

Abstract The band energy scheme of [(CH₃)₂(C₂H₅)₂N][Pd(dmit)₂]₂ at high pressure was discussed and it might be possible that the insulating phase above 7 kbar is related to the 1D metal instability. The low-temperature crystal structures of 2D M(dmit)₂ (M=Ni, Pd) compounds, α-[(CH₃)₂(C₂H₅)₂N]-[Ni(dmit)₂]₂ and (C₇H₁₆N)[Ni(dmit)₂]₂ were determined by imaging plate (IP) system equipped with a closed-cycle helium refrigerator. The X-ray satellite reflections of γ-(EDT-TTF)[Pd(dmit)₂]₂ indicating CDW formation below 80 K were also observed by IP system. [(CH₃)₃HN][Ni(dmise)₂]₂ has a nearly three-dimensional Fermi surface owing to a strong intersheet interaction between their selone groups.

INTRODUCTION

Among π -acceptor molecules M(dmit)₂ (M=Ni, Pd, Pt, ...)(dmit=1,3-dithiole-2-thione-4,5-dithiolate) is only one that has produced molecular superconductors so far. Similar to BEDT-TTF(bis(ethylenedithio)tetrathiafulvalene), M(dmit)₂ molecules are members of a family of multi-chalcogen π molecules.¹

In this paper the low-temperature crystal structures and electronic structures of some representative 1D and 2D M(dmit)₂ conductors and the results about related dmise compounds with 3D Fermi surfaces will be represented.

ELECTRONIC BAND PROPERTIES OF M(dmit)₂ CONDUCTORS

From the viewpoint of molecular design the main difference between organic conductors based on TTF-like π -donor molecules and the conductors based on $M(\text{dmit})_2$ molecules is originated from the difference of the symmetry of the frontier orbitals. Except a few exceptional cases, almost all the $M(\text{dmit})_2$ conductors have columnar structures. When $M(\text{dmit})_2$ molecules form a regular column, the frontier orbital is LUMO (FIG. 1a). This is the case of the $\text{Ni}(\text{dmit})_2$ conductors. Then, the electronic structure tends to be 1D because of the nodal plane of LUMO on central metal atom which strongly diminishes the intermolecular transverse interactions. This is the reason why the simple band structure of the first superconductor $\text{TTF}[\text{Ni}(\text{dmit})_2]_2$ was considered to have one-dimensional nature.² But as pointed out by Canadel, this band picture will be modified when the system is composed of $M(\text{dmit})_2$ dimers and the energy separation (Δ) between LUMO and HOMO is comparable to the sum of the intradimer HOMO...HOMO and LUMO...LUMO interactions.³

Unlike $\text{Ni}(\text{dmit})_2$ salts, the $\text{Pd}(\text{dmit})_2$ (or $\text{Pt}(\text{dmit})_2$) salts have dimerized columns. The intradimer interaction is very strong compared with the interdimer interaction. In this case, the energy level of the dimer state obtained from the bonding combination of LUMOs of two $M(\text{dmit})_2$ molecules ($\epsilon(\text{LUMOs}^+)$) is reduced greatly. While the energy of the state of the anti-bonding combination of HOMOs ($\epsilon(\text{HOMOs}^-)$) will be enhanced. Therefore in the strongly dimerized $M(\text{dmit})_2$ unit, the energy level $\epsilon(\text{LUMOs}^+)$ will become lower than $\epsilon(\text{HOMOs}^-)$ (FIG. 1a). But owing to the large intradimer interaction, the large mid-gap appears and the small interdimer interaction makes the effective band width narrow. Therefore the normal metal behavior cannot be expected even when the tight-binding band calculation gave large Fermi surfaces. Weak temperature dependences of the resistivities frequently observed in $\text{Pd}(\text{dmit})_2$ conductors will be probably related to this band nature. However, at high pressure, the dimeric nature of the $\text{Pd}(\text{dmit})_2$ columns will be diminished and the structure will be thought to become more regular. The energy level inversion between $\epsilon(\text{LUMOs}^+)$ and $\epsilon(\text{HOMOs}^-)$ will be expected to disappear (FIG. 1a).

$[(\text{CH}_3)_2(\text{C}_2\text{H}_5)_2\text{N}][\text{Pd}(\text{dmit})_2]_2$ seems to be a good example of above discussion. Crystal data of $[(\text{CH}_3)_2(\text{C}_2\text{H}_5)_2\text{N}][\text{Pd}(\text{dmit})_2]_2$ is triclinic, space group $P1$, $a=8.218(4)$, $b=18.422(10)$, $c=6.277(3)$ Å, $\alpha=96.76(5)^\circ$, $\beta=115.70(3)^\circ$, $\gamma=90.09(5)^\circ$, $V=848.9(6)$ Å³, $Z=1$.⁴ The $\text{Pd}(\text{dmit})_2$ anions form a strongly dimerized stacks along the $[101]$ direction. The resistivities along the direction parallel to (010) were measured by the four-probe method. The room-temperature conductivity was about 40 S cm^{-1} . Above 2.3 kbar, superconducting transition was observed. It is worth notice that $[(\text{CH}_3)_2(\text{C}_2\text{H}_5)_2\text{N}][\text{Pd}(\text{dmit})_2]_2$ is an anomalous conductor, where an insulating state is stabilized at high pressure (>7 kbar) (FIG. 1b). Usually metallic state appears when superconducting

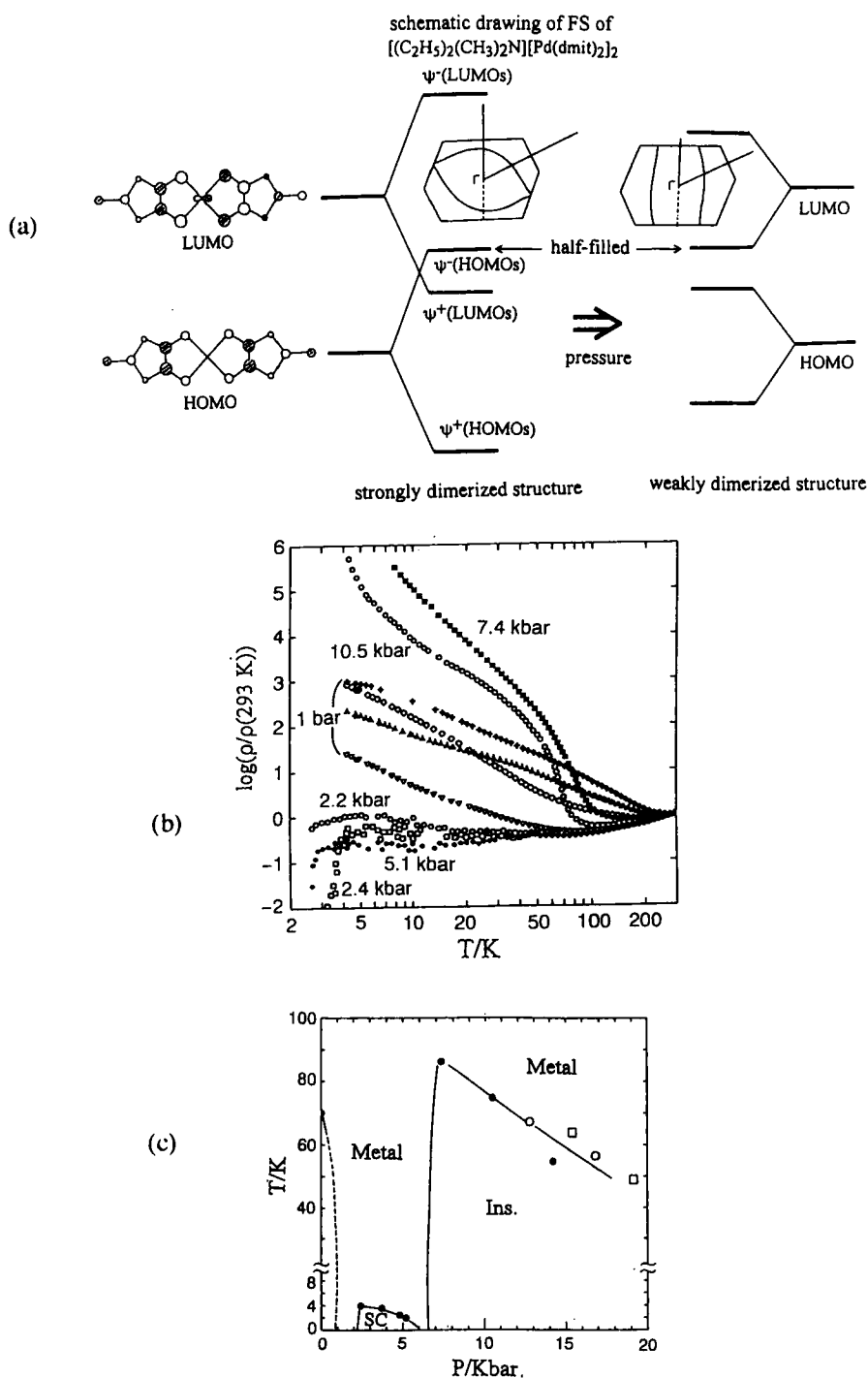


FIGURE 1 (a) Schematic energy diagram of M(dmit)₂ conductors. (b) Temperature and pressure dependences of the resistivities of $[(CH_3)_2(C_2H_5)_2N][Pd(dmit)_2]_2$. (c) A preliminary phase diagram of $[(CH_3)_2(C_2H_5)_2N][Pd(dmit)_2]_2$.

phase disappears at high pressure, because metallic state tends to be stabilized by applying pressure. This may be true if the band nature is not changed at high pressure. It is considered that the dimeric nature of molecular stacks is reduced with increasing pressure, therefore it may be possible that energy level inversion between $\epsilon(\text{LUMOs}^+)$ and $\epsilon(\text{HOMOs}^-)$ disappears at high pressure. If it is a case, the conduction band has the HOMO character at low pressure and the LUMO character at high pressure. Therefore, the dimensionality of the band structure will tend to be diminished from 2D to 1D. Therefore if the inversion of energy levels mentioned before occurs, then the system will exhibit 1D metal instability because $[(\text{CH}_3)_2(\text{C}_2\text{H}_5)_2\text{N}][\text{Pd}(\text{dmit})_2]_2$ has a simple crystal structure, where all the $\text{M}(\text{dmit})_2$ stacks are parallel to each other. A preliminary phase diagram determined from the resistivity measurements is shown in Figure 1c. $[(\text{CH}_3)_2(\text{C}_2\text{H}_5)_2\text{N}][\text{Pd}(\text{dmit})_2]_2$ may be a unique superconductor.

CRYSTAL AND ELECTRONIC STRUCTURES OF 2D $\text{M}(\text{dmit})_2$ CONDUCTORS WITH STACKING(COLUMNAR) STRUCTURES: γ -(EDT-TTF)[$\text{Pd}(\text{dmit})_2$]

γ -(EDT-TTF)[$\text{Pd}(\text{dmit})_2$]

(EDT-TTF)[$\text{Ni}(\text{dmit})_2$] salt has three crystal modifications α , β - and γ - form, while two modifications α' - and γ -form have been found in (EDT-TTF)[$\text{Pd}(\text{dmit})_2$].^{5,7} γ -(EDT-TTF)[$\text{Pd}(\text{dmit})_2$] exhibits a resistivity anomaly below 80 K similar to α -(EDT-TTF)[$\text{Ni}(\text{dmit})_2$] and α' -(EDT-TTF)[$\text{Pd}(\text{dmit})_2$]. Brossard *et al.* reported that temperature dependence of the resistivity of α' -(EDT-TTF)[$\text{Pd}(\text{dmit})_2$] is metallic and exhibits a resistivity peak at ca. 40 K similar to the anomaly of 14K of α -(EDT-TTF)[$\text{Ni}(\text{dmit})_2$].^{5,7} The resistivity anomaly of α' -(EDT-TTF)[$\text{Pd}(\text{dmit})_2$] was suppressed by 5 kbar, but no sign of superconducting transition was found down to 400 mK at 10 kbar.⁷ α' -(EDT-TTF)[$\text{Pd}(\text{dmit})_2$] has crossing columns. The EDT-TTF molecules stack along the [100] direction and $\text{Pd}(\text{dmit})_2$ molecules stack along the [101] direction.

In γ -(EDT-TTF)[$\text{Pd}(\text{dmit})_2$], EDT-TTF and $\text{Pd}(\text{dmit})_2$ molecules form segregated "parallel columns" along the [100] axis. The crystal structure is shown in Figure 2a. The $\text{Pd}(\text{dmit})_2$ molecules form a dimeric column. The interplanar distance within a dimer is 3.174 Å and interdimer distance is 3.813 Å. In γ -(EDT-TTF)[$\text{Pd}(\text{dmit})_2$] two $\text{Pd}(\text{dmit})_2$ anions adopt an eclipsed configuration within a dimer (A) and are displaced sideways with respect to each other between dimers(B). EDT-TTF molecules form a weak dimer along the [100] axis, the intradimer distance is 3.552 Å(A) and the interdimer distance is 3.786 Å(B).

The anisotropy of the electrical resistivities of γ -(EDT-TTF) [Pd(dmit)₂] under the high pressure were measured within the temperature range of 300 K to 2K (FIG. 2b). The resistivity measured perpendicular to the [101] direction showed that it decreased down to 100 K and increased below 80 K, having round maximum around 50 K. The resistivity measurement along the [101] direction showed the metal-semimetal transition around 50 K. This resistivity anomaly which was observed perpendicular to the [101] direction decreased when the pressure increased. Above 10 kbar the resistivity anomaly was suppressed and the metallic region appeared. No sign of superconductivity was found down to 1.5 K and up to 12 kbar.

In order to examine the origin of the metal instabilities of γ -(EDT-TTF)[Pd(dmit)₂] below 80 K, the X-ray diffuse scattering experiments were made. The crystal structure studies at 13 K were performed by Weissenberg type low-temperature IP (imaging plate) system equipped with closed cycle helium refrigerator. The oscillation photographs were taken around the b-axis. At 300 K no satellite reflections were observed. The resistivity anomaly appeared around 80 K and a little above 100K very faint extra diffuse reflections were observed. At 80 K clear satellite reflections were observable. The satellite reflections grew along the direction of the [101] axis. Figure 2c shows P, Q satellite reflections on the direction of the [101] axis at 30 K. Thus in γ -(EDT-TTF)[Pd(dmit)₂] the resistivity increase around 80K is due to the development of CDW with the wave vector of $q=0.41(a^*+c^*)$. The intensities of the satellite reflections began to increase at 80 K, where the resistivity anomaly began to increase. Figure 2d shows the increasing of the intensity of P, Q satellite reflections. This resistivity anomaly should be associated with a CDW instability of the EDT-TTF or Pd(dmit)₂ chain. However, in one-dimensional conductors satellite reflections usually appear at a temperature fairly higher than the transition temperature. In this system no diffuse streaks or diffuse spots were observed from high temperature, that indicates this system is not one-dimensional but rather two-dimensional. The crystal structure determination of γ -(EDT-TTF)[Pd(dmit)₂] by IP system were performed at 18K.

CRYSTAL AND ELECTRONIC STRUCTURES OF 2D M(dmit)₂ CONDUCTORS WITH "SPANNING OVERLAPPING MODE OF MOLECULAR ARRANGEMENT": α -[(CH₃)₂(C₂H₅)₂N][Ni(dmit)₂]₂ AND (C₇H₁₆N)[Ni(dmit)₂]₂

α -[(CH₃)₂(C₂H₅)₂N][Ni(dmit)₂]₂

Black plate crystals of [(CH₃)₂(C₂H₅)₂N][Ni(dmit)₂]₂ were prepared by electrochemically.^{6,8} X-Ray examination showed the existence of three modifications (α , β and γ). The resistivity measurements revealed that α and γ type

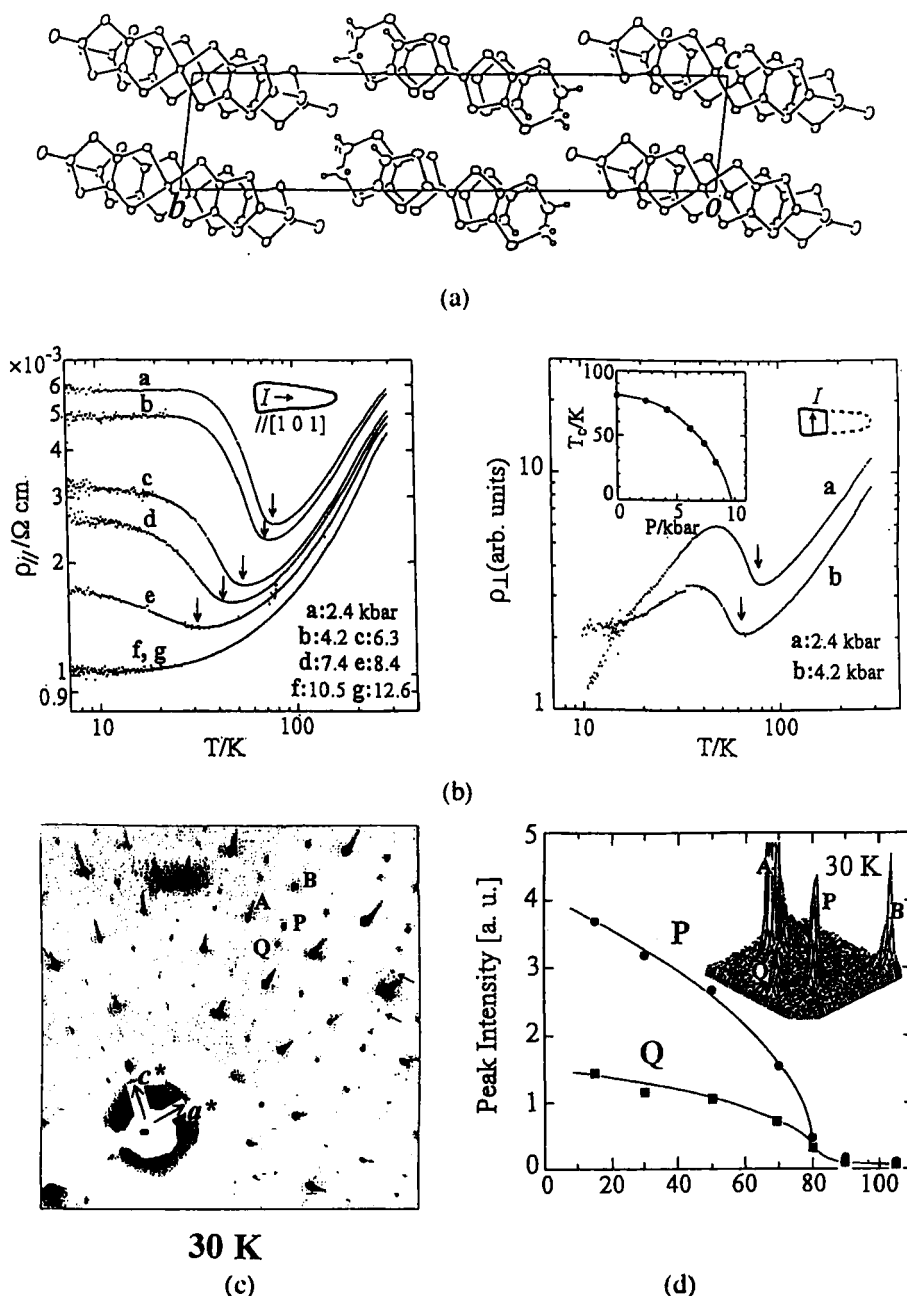


FIGURE 2 (a) Crystal structure of γ -(EDT-TTF)[Pd(dmit)₂]₂. Both EDT-TTF and Pd(dmit)₂ molecules stack along the [100] axis, forming parallel columns. (b) The anisotropy of the resistivity of γ -(EDT-TTF)[Pd(dmit)₂]₂ under the high pressure. Current is perpendicular to [101] (right); current is parallel to [101] (left). (c) Oscillation photographs of γ -(EDT-TTF)[Pd(dmit)₂]₂ along the [101] axis. (d) Increasing of the intensities of satellite reflections of P and Q at 30 K.

crystals to be metallic and β type one semiconducting. Crystals with smooth resistivity decrease were revealed to be γ -type ones. The others with the 240 K anomaly were α -type crystals (FIG. 3a).⁷ The resistivity jump around 240 K was due to the cracks of the crystal produced by the drastic structural phase transition.

The crystal structure determination at 11 K was performed by the IP system. An extremely large discontinuous lattice contraction was observed at 240 K along the a axis ($\Delta a = -1.24$ Å). The lattice constants c and β also exhibited discontinuous change ($\Delta c = +0.11$ Å, $\Delta\beta = 5.5^\circ$). In contrast, a continuous change was observed along the b direction, along which Ni(dmit)₂ molecules are arranged closely side-by-side.² The X-ray diffraction patterns clearly showed the change of the extinction rule, indicating the transformation from the base-centered lattice(C) to the primitive lattice(P).

The space group of $C2/c$ of high-temperature phase is changed to $P2_1/c$. The crystal data are : monoclinic, $C2/c$, $a=38.95(2)$ Å, $b=6.494(2)$, $c=13.835(9)$, $\beta=99.63(5)^\circ$, $V=3454(1)$ Å³, $Z=4$ at room temperature and monoclinic, $P2_1/c$, $a=37.499(12)$ Å, $b=6.444(2)$, $c=13.718(5)$, $\beta=92.69(2)^\circ$, $V=3311.2(2)$ Å³, $Z=4$ at 11 K. The crystal structure is not a simple 1D column structure(FIG. 3b). Along the b -axis, [Ni(dmit)₂] anions are arranged in a side-by-side fashion with short S...S distances. In the c direction, Ni(dmit)₂ anions show two types of overlap, one of which is "spanning overlap"^{5,6}(FIG. 3c). Spanning overlap is a stacking motif that one molecule overlaps with two molecules. As was expected, (CH₃)₂(C₂H₅)₂N cation on the general position, which was on the twofold axis and disordered at room temperature, becomes ordered at 11 K. In the room-temperature structure, there exists a short interlayer S...S contact (3.352 Å) between terminal thionyl S atoms of Ni(dmit)₂ molecules. This S...S contact was expected to become shorter at low temperature. However unexpectedly, in spite of the extremely large shortening of the a axis, it becomes longer (3.463 Å). Therefore the interlayer interaction becomes very small and the "three-dimensionality" is negligible at low temperature.

According to the simple extended Huckel tight-binding approximation, the band structure calculated on the basis of the room-temperature structure with $C2/c$ space group gave two-dimensional Fermi surface similar to that of the superconductors with κ -type molecular arrangement with close crosssectional area of 100% of BZ⁹.

However, the Fermi surface obtained from the angular dependent magnetoresistance oscillation and Shubnikov-de Haas (SdH) effect did not coincide with the results of this band calculation.

The extended Huckel tight-binding band of α -[(CH₃)₂(C₂H₅)₂N] [Ni(dmit)₂]₂ based on the 11 K structure and x-ray evidence of the twofold superlattice at low temperature gave complex 2D Fermi surfaces(FIG.3d), which agree well with those

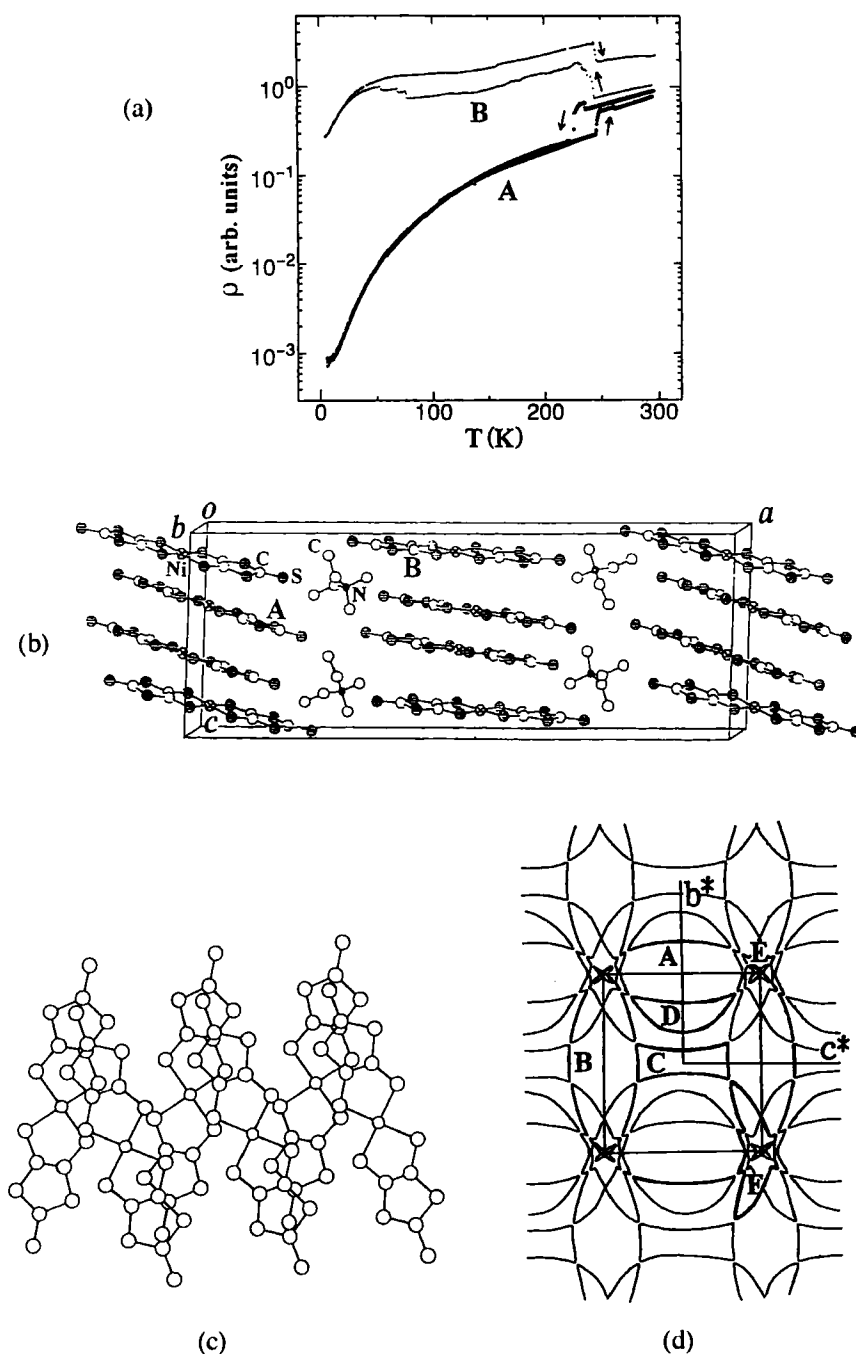


FIGURE 3 (a) Temperature dependence of the resistivities of α -[$(\text{CH}_3)_2(\text{C}_2\text{H}_5)_2\text{N}$] [Ni(dmit) $_2$] $_2$. (b) The 11-K structure of α -[$(\text{CH}_3)_2(\text{C}_2\text{H}_5)_2\text{N}$] [Ni(dmit) $_2$] $_2$. (c) The spanning overlap mode. (d) Fermi surface calculated by the 11-K structure.

expected from magnetoresistance experiments. This shows that the simple extended Huckel band calculation, which has been successfully applied to organic metals, is also valid for the evaluation of the Fermi surfaces of the molecular metals based on transition-metal-complex molecules.

(C₇H₁₆N)[Ni(dmit)₂]₂

(C₇H₁₆N)[Ni(dmit)₂]₂ is isomorphous to α -[(CH₃)₂(C₂H₅)₂N][Ni(dmit)₂]₂ and is metallic down to 0.5 K.¹¹ α -[(CH₃)₂(C₂H₅)₂N][Ni(dmit)₂]₂ has a resistivity jump around 240 K, however resistivity curve of (C₇H₁₆N)[Ni(dmit)₂]₂ has a bend around 225 K. According to the simple extended Huckel tight-binding approximation, the band structure calculated on the basis of the room temperature structure gave two-dimensional Fermi surface similar to that of the first κ -type superconductor, κ -(BEDT-TTF)₂I₃.¹² Similar to α -[(CH₃)₂(C₂H₅)₂N][Ni(dmit)₂]₂, (C₇H₁₆N)[Ni(dmit)₂]₂ has a structure "spanning overlap" at room temperature. The low temperature crystal structure was examined from 300K to 20K by the Weissenberg type low-temperature IP system. Below 225 K, the satellite reflections indicating fivefold superstructure along the b axis were observed. The space group of C2/c of the high-temperature phase is changed to Cc at 20 K. The crystal data are: a=39.014(15), b=6.483(2), c=13.806(5) Å, β =96.62(1)°, V=3468.8 Å³, Z=4 at room temperature. a=39.01(1), b=32.20(1), c=13.545(4) Å, β =96.36(2)°, V=16910 Å³, Z=20 at 20 K. The crystal structure at 20 K are shown in Figure 4a. The C₇H₁₆N⁺ cations are on the two fold axis and thus at room temperature they are heavily disordered. The crystal structure has transformed to fivefold structure along the b axis at 20 K. Although there still remain positional disorder at 20 K, the C₇H₁₆N⁺ cation sites were satisfactorily determined. The arrangement of C₇H₁₆N⁺ cations are shown in Figure 4b. Roughly speaking, the cations take two kinds of orientations (α and β). Along the b axis the orientations of cations were determined approximately α , α , β , β and $\alpha\beta$ (disorder). In order to cancel the polarity of the cations and maintain the c-glide symmetry, a stacking disorder along the b axis is expected. The diffuse sheet which indicates the stacking disorder along the b axis was observed in the oscillation photographs at 20 K.

Crystal structure and electronic structure of 3D metallic M(dmise)₂ compounds: [(CH₃)₃HN][Ni(dmise)₂]₂ and (EDT-TTF)[Ni(dmise)₂]

Besides dmit ligand, dmise(dmise=4,5-dimercapto-1,3-dithiole-2-selone) including both sulfur and selenium atoms, is a potentially useful ligand which extends an intermolecular interaction towards the third direction through its outstretched part of

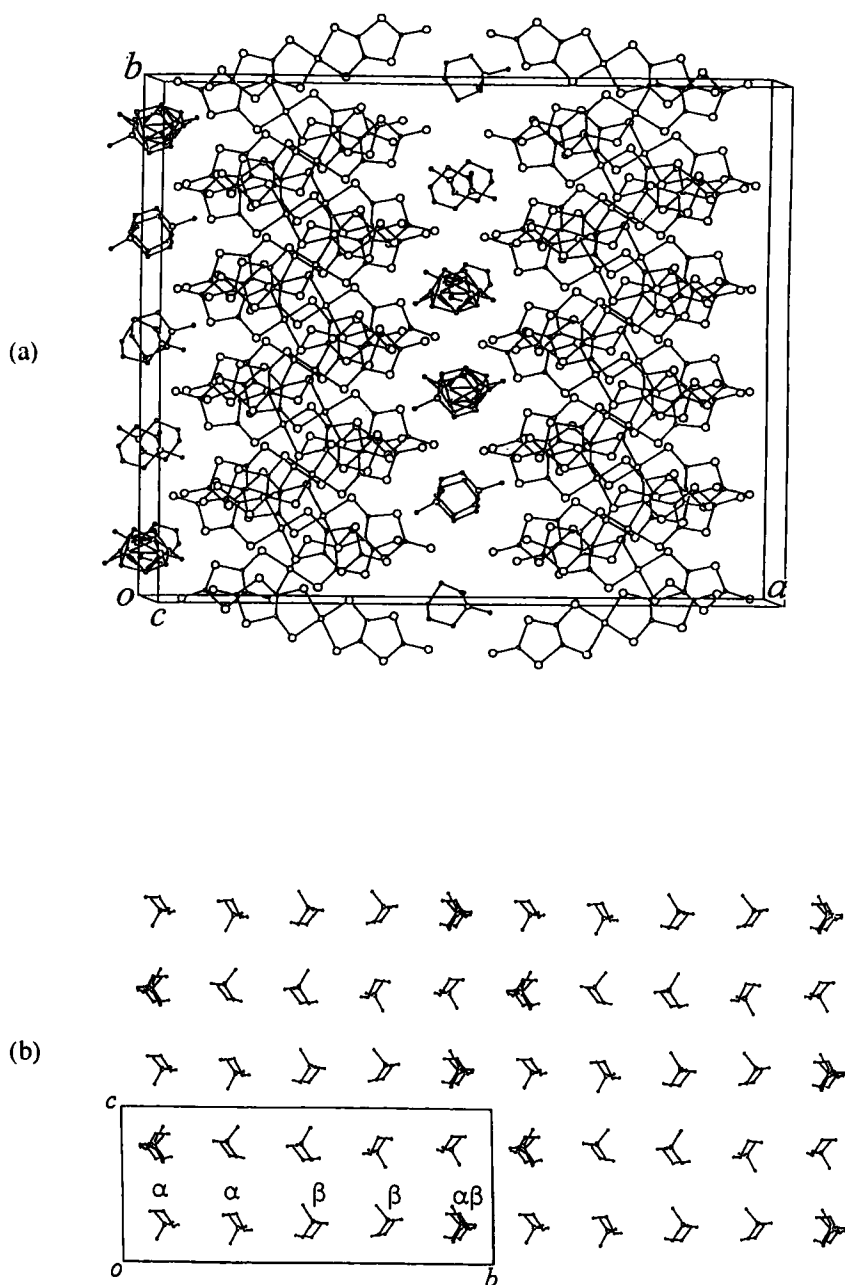


FIGURE 4 (a) The crystal structure of $(\text{C}_7\text{H}_{16}\text{N})[\text{Ni}(\text{dmit})_2]_2$. (b) The arrangement of cations in $(\text{C}_7\text{H}_{16}\text{N})[\text{Ni}(\text{dmit})_2]_2$.

its π -conjugation system, *i.e.* the selone. Cornelissen et al. reported two $(\text{CH}_3)_4\text{N}^+$ salts.¹³ $[(\text{CH}_3)_3\text{HN}][\text{Ni}(\text{dmise})_2]_2$ exhibits weakly metallic behavior around room temperature with a conductivity of 100 S cm^{-1} , the resistivity gradually increases at low temperatures, the activation energy is 0.005 eV .¹⁴ The insulating phase is not completely suppressed even at 6 kbar. $(\text{EDT-TTF})[\text{Ni}(\text{dmise})_2]$ also exhibited metallic conductivity around room temperature and made a smooth transition into an insulator at low temperature.

The crystal data of $[(\text{CH}_3)_3\text{HN}][\text{Ni}(\text{dmise})_2]_2$ are: triclinic, $P1$, $a=7.606(3)$, $b=17.761(3)$, $c=6.660(2) \text{ \AA}$, $\alpha=100.27(2)$, $\beta=114.93(2)$, $\gamma=81.84(2)^\circ$, $V=800.4(4) \text{ \AA}^3$, $Z=1$. The $\text{Ni}(\text{dmise})_2$ molecules stack along the a -axis almost regularly, interplanar distances are 3.464 and 3.557 \AA . The most striking feature is that there are also found short contacts of $\text{Se}\cdots\text{Se}$ (3.486 and 3.801) through the cation sheet, which is also observed in $\alpha-[(\text{CH}_3)_4\text{N}][\text{Ni}(\text{dmise})_2]_2$ (3.277 \AA).¹² The tight binding band calculation by extended Huckel methods indicated that $[(\text{CH}_3)_3\text{HN}][\text{Ni}(\text{dmise})_2]_2$ has even stronger intermolecular interactions along the long molecular axis than the transverse direction owing to a close selenium-selenium contact. This feature leads to a 3D electronic structure (FIG. 5) indicating this complex to be a precursor of 3D molecular metal based on planar π -conjugated molecules. $[(\text{CH}_3)_2\text{H}_2\text{N}][\text{Ni}(\text{dmise})_2]_2$ with similar 3D Fermi surface could be also obtained. The $\text{M}(\text{dmise})_2$ salt has demonstrated that intermolecular interaction was expanded towards the third direction by the substitution of the selone group for the thione group.

The X ray-structural analysis of $(\text{EDT-TTF})[\text{Ni}(\text{dmise})_2]$ has not yet been completely satisfactory because a crystal of high enough quality has not been available. Crystal data: triclinic, $P1$, $a=23.43$, $b=6.47$, $c=4.23 \text{ \AA}$, $\alpha=86.8$, $\beta=90.2$, $\gamma=95.1^\circ$, $V=637.2 \text{ \AA}^3$, $Z=1$. The donor EDT-TTF and acceptor $\text{Ni}(\text{dmise})_2$ molecules make segregated columns, running in parallel with each other along the $[001]$ direction.

By a similar synthetic method we obtained single crystals (thin plates or needles) of $(\text{CH}_3)_x(\text{C}_2\text{H}_5)_{4-x}\text{N}$ ($x=0-4$) salts of $\text{Ni}(\text{dmise})_2$ and $\text{Cs}[\text{Pd}(\text{dmise})_2]_2$. $\text{Cs}[\text{Pd}(\text{dmise})_2]_2$ is the only $\text{M}(\text{dmise})_2$ compound which has metallic conductivity down to 4 K .

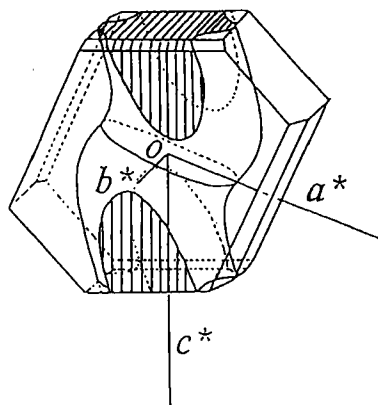


FIG. 5. Schematic view of the Fermi surface of $[(CH_3)_3HN][Ni(dmisc)_2]_2$.

REFERENCES

- 1 L. Brossard, M. Ribault, L. Valade and P. Cassoux, *Physica B & C*(Amsterdam), **143** 378 (1986) ; A. Kobayashi, H. Kobayashi, A. Miyamoto, R. Kato, R. A. Clark and A. E. Underhill, *Chem. Lett.*, **1991**, 2163. ; P. Cassoux, L. Valade, H. Kobayashi, A. Kobayashi, R. A. Clark and A. E. Underhill, *Coord. Chem. Rev.*, **110**, 115 (1991).
- 2 A. Kobayashi, H. Kim, Y. Sasaki, R. Kato and H. Kobayashi, *Solid State Commun.*, **62**, 57 (1987).
- 3 E. Canadell, E.I. Rachidi, S. Ravy, J.-P. Pouget, L. Brossard and J.-P. Legros, *J. Phys. (Paris)*, **50**, 2967 (1989).
- 4 H. Kobayashi, K. Bun, T. Naito, R. Kato and A. Kobayashi, *Chem. Lett.*, **1992**, 1909; A. Kobayashi, R. Kato, R.A. Clark, A.E. Underhill, A. Miyamoto, K. Bun, T. Naito and H. Kobayashi, *Syn. Met.* **55-57**, 2927 (1993).
- 5 A. Kobayashi, A. Sato, K. Kawano, T. Naito, H. Kobayashi and T. Watanabe, *J. Mater. Chem.*, **5**, 1671 (1995); R. Kato, H. Kobayashi, A. Kobayashi, T. Naito, M. Tamura, H. Tajima and H. Kuroda, **1989**, 1839.
- 6 R. Kato, H. Kobayashi, H. Kim, A. Kobayashi, Y. Sasaki, T. Mori, and H. Inokuchi, *Chem. Lett.*, **1988**, 865.
- 7 B. Garreau, B. Pommarede, C. Faulmann, J.-M. Fabre, P. Cassoux, J.-P. Legros, *C.R. Acad. Sci. Paris, Ser. II*, **313**, 509 (1991); L. Brossard, M. Ribault, B. Garreau, B. Pommarede, P. Cassoux, *Europhys. Lett.*, **19**, 223 (1992).
- 8 A. Kobayashi, T. Naito and H. Kobayashi, *Phys. Rev.* **B51**, 3198 (1995).
- 9 H. Tajima, S. Ikeda, M. Inokuchi, A. Kobayashi, T. Ohta, T. Sasaki, N. Toyota, R. Kato, H. Kobayashi and H. Kuroda, *Solid State Commun.*, **88**, 605 (1993).
- 10 A. Kobayashi, T. Naito and H. Kobayashi, to be published.
- 11 A. Kobayashi *et al.* to be published.
- 12 A. Kobayashi, R. Kato, H. Kobayashi, S. Moriyama, Y. Nishio, K. Kajita and W. Sasaki, *Chem. Lett.*, **1987**, 459.
- 13 J. P. Cornelissen, B. Pommarede, A.L. Spek, D. Reefman, J. G. Haasnoot, J. Reedijk, *Inorg. Chem.*, **32**, 3720 (1993).
- 14 T. Naito, A. Sato, K. Kawano, A. Tateno, H. Kobayashi and A. Kobayashi, *J. C.S. Chem. Commun.*, **1995**, 351.